Journal of Molecular Structure 997 (2011) 78–86

Contents lists available at ScienceDirect

Journal of Molecular Structure

journal homepage: www.elsevier.com/locate/molstruc

Structural investigation of chitosan-based microspheres with some anti-inflammatory drugs

Simina Dreve [a], Iren Kacso [a], Adriana Popa [a], Oana Raita [a], Felicia Dragan [b], A. Bende [a], Gh. Borodi [a], I. Bratu [a,*]

[a] National Institute for R&D of Isotopic and Molecular Technologies, 65-103 Donáth st., RO-400293 Cluj-Napoca, Romania
[b] University of Oradea, Faculty of Medicine and Pharmacy, 54 N. Jiga st., Oradea, Romania

ARTICLE INFO

Article history:
Received 5 April 2011
Received in revised form 3 May 2011
Accepted 3 May 2011
Available online 14 May 2011

Keywords:
Chitosan
Microspheres
Anti-inflammatory drugs
Molecular spectroscopy

ABSTRACT

The use of chitosan as an excipient in oral formulations, as a drug delivery vehicle for ulcerogenic anti-inflammatory drugs and as base in polyelectrolyte complex systems, to prepare solid release systems as sponges was investigated. The preparation by double emulsification of chitosan hydrogels carrying diclofenac, acetyl-salycilic acid and hydrocortisone acetate as anti-inflammatory drugs is reported. The concentration of anti-inflammatory drug in the chitosan hydrogel generating the sponges was 0.08 mmol. Chitosan-drug loaded sponges with anti-inflammatory drugs were prepared by freeze–drying at −60 °C and 0.009 atm. Structural investigations of the solid formulations were done by Fourier-transformed infrared and ultraviolet-visible spectroscopy, spectrofluorimetry, differential scanning calorimetry and X-ray diffractometry. The results indicated that the drug molecules are forming temporary chelates in chitosan hydrogels and sponges. Electron paramagnetic resonance demonstrates the presence of free radicals in a wide range and the antioxidant activity for chitosan-drug supramolecular cross-linked assemblies.

1. Introduction

The concept of designing a specified delivery system has been originated from the perception of Paul Ehrlich, who proposed drug delivery to be as a 'magic bullet' [1], where a drug-carrier complex/conjugate, delivers drug(s) exclusively to the preselected target cells in a specific manner. The objective of drug targeting is to achieve desired pharmacological response at a selected site without undesirable interactions. It is well known that most of anti-inflammatory drugs administered in therapeutic doses, increase the sensitivity of the gastric mucosa against the aggressive factor, and the acid can produce gastro-intestinal inflammations or ulcers [2]. Between natural polymers generating novel biomaterials, chitin and chitosan with their copolymers, are intensively studied due to their many potential applications. Chitosan [poly(b-(10/4)-2-amino-2-deoxy-Dglucose)] (CTS) is a natural cationic polysaccharide derived from chitin, which is copolymer, a glucosamine and an N-acetyl glucosamine units, combined together [3]. Chitosan is being widely used as a pharmaceutical excipient, comprising a series of polymers varying in their degree of deacylation, molecular weight, viscosity, *pKa*, etc. The presence of a number of amino groups permits CTS to chemically react with anionic systems, thereby resulting in alteration of physicochemical characteristics of reactants and developing new properties of such combinations [4]. Moreover, chitosan has antiacid and antiulcer characteristics, which prevents or weakens drug irritation in the stomach [5]. Modern biocompatible systems target not only infectious diseases, but also autoimmune disorders, allergies, chronic inflammatory diseases and cancer [6]. Small molecular weight anti-inflammatory drugs that contain chemical groups able to establish temporary physical or chemical bonding with the amino group of the CTS linkage are suitable for the targeted and controlled drug CTS-based delivery systems. In support of this presumption the chemical formulae of CTS, additives and anti-inflammatory drugs used in the experiment are illustrated in Fig. 1. The present study was aimed to develop and characterize a CTS novel solid complex with Tween-80 and oleic acid as drug carrier for controlled drug delivery, with possible use in controlled (slow) drug delivery, avoiding gastrointestinal painful injuries. The hydrogel poly-electrolyte complexes of chitosan (PEC CTS) were prepared by double emulsification and coacervation method using the 0.02% Tween-80, 0.02% oleic acid in 3% CTS acidic solution [7]. Diclofenac sodium (DCF-Na) and acetyl-salycilic acid (ASA) are among the most useful non-steroidal anti-inflammatory drugs (NSAIDs). Both, and the steroidal anti-inflammatory drug hydrocortisone acetate (HcAc) too, dissolve in gastro-intestinal fluid [8,9] causing gastric mucosal damage. The *pH* of the gastrointestinal tract (GIT) varies from *pH* 1 to 3 in the stomach and increases to approximately 7–8 in the colon. Another factor influencing the activity of drugs are the struc-

* Corresponding author. Tel.: +40 264 584037; fax: +40 264 420042.
E-mail address: ibratu@gmail.com (I. Bratu).

0022-2860/$ - see front matter © 2011 Elsevier B.V. All rights reserved.
doi:10.1016/j.molstruc.2011.05.001

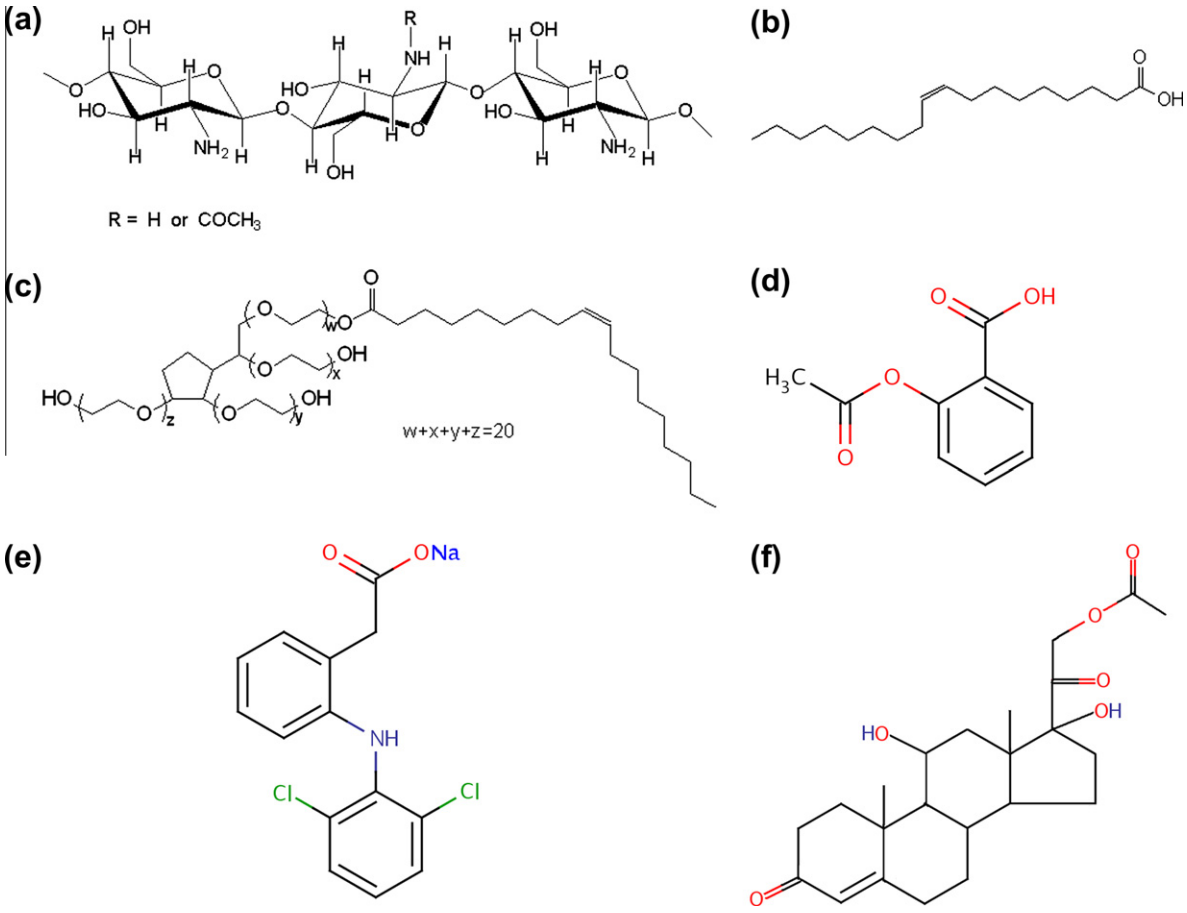

Fig. 1. Structural formula of: (a) chitosan, (b) oleic acid, (c) Tween 80, (d) acetyl-salycilic acid, (e) diclofenac sodium, (f) hydrocortison acetate.

tural changes they can have in digestive tract, for example diclofenac is suffering an intramolecular cyclization under acidic conditions, which causes the salt to become inactivated [10]. An important advantage of anti-inflammatory microencapsulated systems in chitosan as active substance carrier include polymeric shell protection against degradation factors like *pH* and light and the reduction of tissue irritation due to the polymeric shell [11,12]. The structural formulae of chitosan and of the drugs used in this study are represented in Fig. 1.

2. Materials and methods

2.1. Materials

Chitosan from crab shells with 85% deacetylation degree, oleic acid and respectively Tween-80 were purchased from Sigma Aldrich GmbH (Chitosan: product number 448877; Oleic acid: product number O1008; Tween-80: product number P4780). Diclofenac sodium (DCF-Na) was obtained from "*Terapia Ranbaxy*" *S.A.* Cluj-Napoca (Romania), acetyl-salycilic acid (ASA) was obtained from "*Helcor*" *s.r.l.* Baia Mare (Romania) and hydrocortisone acetate (HcAc) was obtained from *Bayer* GmbH, all having purity of pharmaceutical grade (>99.99%). All these chemicals were used without further purification.

2.2. Preparation of CTS-base solution

CTS poly-electrolyte (PEC) hydrogel 0.25% was prepared in double distilled water containing 1% (v/v) acetic acid with continuous stirring at 30 °C, adding at final 0.02% v/v Tween-80 and 0.02% v/v oleic acid. After 6 h the solution is pale-yellow, with a homogenous consistence and aspect.

2.3. Preparation of CTS-based drug loaded nano/microparticles

To the CTS poly-electrolyte solution, split in 12 equal volumes, 10 ml each, solutions of anti-inflammatory drugs in ethylic alcohol: double distilled water 1:1 were added, to give final solutions with 0.08 mmol active drug. Finally three solutions of each CTS-drug system, and three blank solutions were obtained, all experimental testing were performed in parallel for each drug. The solutions were further stirred for 30 min and then ultrasonically treated in an Elmasonic E60H ultrasonic bath for 10 min, resulting nanostructured (n-CTS) and microstructured chitosan (μ-CTS) in the PEC solution. In order to prepare the sponges the hydrogels were freeze–dried in a CHRIST ALPHA 1-4 LD Plus Freeze Dryer, at −60 °C and 0.09 atm.

2.4. Instrumentation

The morphologic analysis was performed by examining the PEC hydrogel with the IR JASCO IRT-3000 microscope, an accessory of the FTIR 6100 spectrometer.

UV–Vis spectroscopy was performed for liquid PEC hydrogels in the range 200 nm–900 nm, using the spectrophotometer ABLE & JASCO 550 V.

The fluorescence spectra due to the interactions between drugs and chitosan were studied on solid samples using a ABLE & JASCO FP 6500 recording spectrofluorometer, applying an excitation

wavelength of 230 nm and monitoring the emission wavelength over the 250–440 nm range. Both excitation and emission slit openings were set at bandwidths of 3 μm.

FTIR spectra were obtained with a JASCO 6100 FTIR spectrometer in the 4000–400 cm^{-1} spectral domain with a resolution of 4 cm^{-1} by using KBr pellet technique.

The DSC thermograms were obtained with a DSC-60 Shimadzu differential scanning calorimeter. The samples' heating was done with a rate of 10 °C/min in the 20–500 °C interval by using sealed Al cells, in nitrogen atmosphere. An empty cell was taken as reference.

Electron spin resonance (ESR) measurements were carried out in the X-band at room temperature using a Bruker E-500 ELEXSYS spectrometer. The spectra processing was performed by Bruker Xepr software.

X-ray diffractograms were obtained with a Bruker D8 Advance diffractometer in the $2\theta = 2–50°$ angular domain using Cu $K\alpha_1$ radiation. In order to increase the resolution a monochromator was used to eliminate the $K\alpha_2$ radiation.

The molecular modeling calculations were performed using the density functional-based tight binding method combined with the self-consistent charge technique (SCC-DFTB), including the empirically correction for dispersion and implemented in the DFTB program code.

3. Results and discussion

3.1. Morphologic characterization of CTS-based drug loaded hydrogel

In order to evidence PEC nano- and micro-spheres obtained after sonication, the FTIR microscopy images are presented in Fig. 2. As one side of the image is 200 μm, we can assume that the microparticles have dimensions of tenths of micrometers.

3.2. UV–Vis spectroscopy

The analysis of UV–Vis spectra, see Fig. 3, revealed characteristic absorption peaks, indicating the encapsulation of ASA, DCF-Na and HcAc, respectively in CTS matrix. Data with the characteristic absorption bands are presented in Table 1.

In the spectra of chitosan an intense maximum at 234 nm and a small peak at 275 nm can be observed. Under the influence of drugs a combined hyperchromic and batochromic effect of chitosan maxima appears, suggesting that between CTS matrix and anti-inflammatory drug physical–chemical stable bonds are established [13]. A low hyperchromic effect is found for CTS/HcAc system, suggesting that the hydrocortisone molecule is less integrated in the chitosan PEC system, due to its larger dimensions as compared with DCF or ASA.

3.3. Spectrofluorimetric analysis

The emission spectra for the specified drugs and their solid samples with n-CTS and μ-CTS obtained by freeze–drying are presented in Fig. 4.

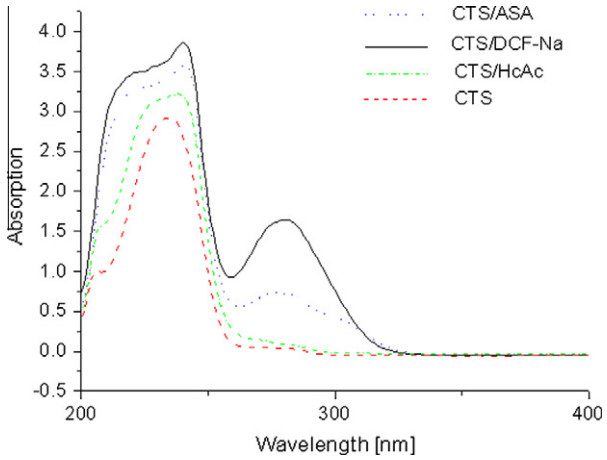

Fig. 3. UV–Vis spectra of ASA, DCF-Na and HcAc, respectively in CTS matrix.

Table 1
Absorption peaks of CTS, and anti-inflammatory drugs ASA, DCF-Na, HcAc, and of their complex hydrogels.

Examined substance/assembly	Wavelenght (nm)
CTS	234
ASA	202, 232.6
DCF-Na	202, 233
HcAc	202, 232.6, 260.7, 299
CTS/ASA	241, 277
CTS/DCF-Na	240, 279.5
CTS/HcAc	238, 275

The analysis of the spectra obtained from the fluorescence measurements (Fig. 4) reveals the increase of fluorescence intensity in CTS/ASA, and a decrease in intensity CTS/DCF-Na and CTS/HcAc respectively, in report with pure drugs spectra. This effect can be explained by the penetration of the drug molecule in chitosan network, activating carboxylic and hydroxilic sites and establishing physical–chemical interactions in the composite. It can be assumed that the interactions in the composite cover the whole range from electrostatic interactions to hydrogen bonds, and finally the establishment of peptide links between carboxylic groups of the drug and unprotected amino-groups of chitosan [14]. Examining the fluorescence spectra, it can be observed that the most intense fluorescence band is for CTS/ASA and increased in comparison with the fluorescence of pure ASA. The different behavior of fluorescence in comparison with that corresponding to CTS/DCF-Na and CTS/HcAc, can be attributed to the difference in molecular mass and between the stereochemistry of the three drugs, in report with chitosan network. In consequence aspirin molecule can penetrate chitosan network, can establish peptide linkage, integrating in the network, and exposing to fluoresce new active sites in the chain. Another explanation is the conformational change of CTS chain and network, as in drugs, which appears when drugs are included in chitosan network and the exposition of active sites to excitation more

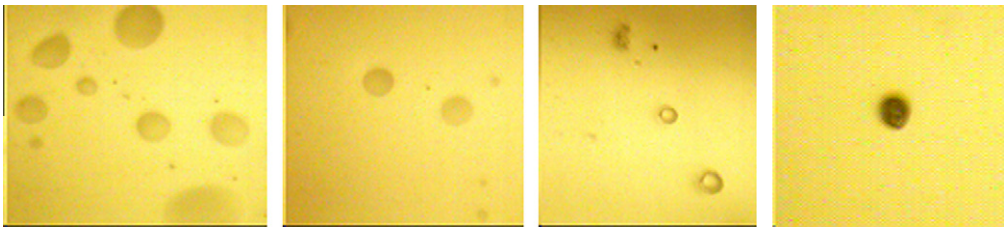

Fig. 2. Optical microscopy images for chitosan hydrogel drug loaded vesicles (0.08 mmol active drug). The dimensions of the image are 200 × 200 μm.

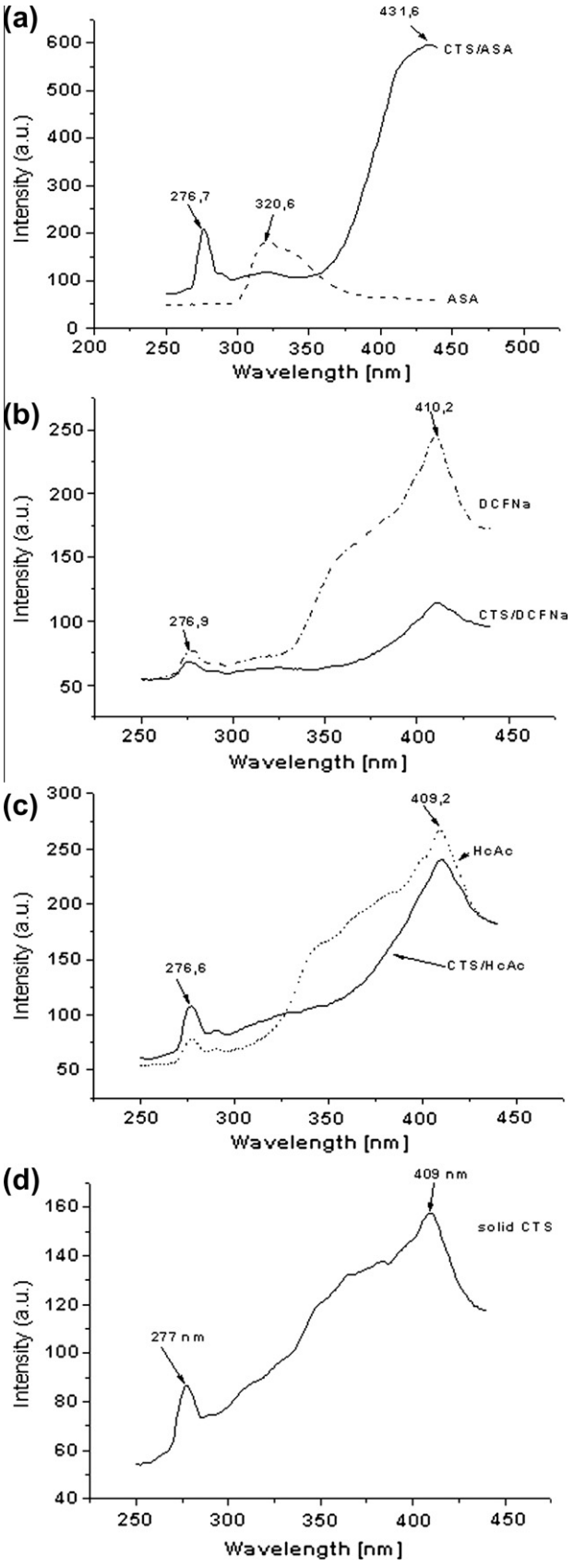

Fig. 4. The emission spectra for the solid samples with n-CTS and μ-CTS obtained by freeze–drying: (a) chitosan with acetyl-salycilic acid, (b) chitosan with diclofenac sodium; (c) chitosan with hydrocortison acetate, (d) chitosan.

easily. In the same scenario DCF-Na or HcAc cannot integrate so easily due to their bigger molecules and, in the same time, due to their more pronounced amphiphilic character (see Table 2).

3.4. Fourier transform infrared (FTIR) spectral studies

The assignment of the most intense bands of CTS on going from higher frequencies, see Table 1 of Ref. [15] 3450 cm^{-1} (amine N—H symmetric stretching); 2929 cm^{-1} (aliphatic C—H stretching), 3440 cm^{-1} (O—H stretching), 2919 cm^{-1} and 2845 cm^{-1} (C—H stretching), 1410 cm^{-1} and 1380 cm^{-1} (CH_3 asym and sym stretching, respectively), 1650 cm^{-1} (amide I), 1594 cm^{-1} (amide II), 1379 cm^{-1} (amide III), 1355 cm^{-1} (O—H bending), 1145 cm^{-1} (C—O—C stretching) 1100 and 1073 cm^{-1} (C—O stretching), 1050 and 1020 cm^{-1} (intramolecular C—O stretching) (see Figs. 5 and 6).

In the case of acetylsalicylic acid (aspirin) the most characteristic vibrational modes of functional molecular groups were located at: 1770-1800 cm^{-1} (esters with phenyl group), 1680–1700 cm^{-1} (C=O stretching in acyl acid) and 1230–1250 cm^{-1} (acetates) [16].

In the case of ASA system the frequency massif of 3437 cm^{-1} in pure CTS is shifted to 3453 cm^{-1} for the CTS/ASA system. The ester stretching at 1753 cm^{-1} in pure ASA is shifted to 1736 cm^{-1} for CTS/ASA system. Also, the carboxylic C—O ester located at 1189 cm^{-1} in ASA spectrum is shifted at 1196 cm^{-1} in the CTS/ASA spectrum.

Based on vibrational analysis of diclofenac [17,18] the most intense IR frequencies have been assigned as follows: ν(NH) is located at 3388 and 3260 cm^{-1}, whereas the ν_{as}(COO) and ν_{sym}(COO) are found at 1572 and 1402 cm^{-1}, respectively. The asymmetric ν_{as}(COO) band is shifted to 1580 cm^{-1} in the CTS/DCF-Na spectrum. As concerned the Hydrocortisone acetate, its infrared characteristic frequencies, see Table 5 of Ref. [19] are located at: 1406 cm^{-1} (C—H deformation of 2-CH_2 group, 1328, 1273, 1233, 1195, 1017, 950, 942 and 880 cm^{-1} (C—H out-of-plane deformation, respectively. C=O stretching vibration located at 1746 and 1721 cm^{-1} in HcAc spectrum is shifted to 1744 cm^{-1} in CTS/HcAc spectrum. The C=C stretching at 1629 cm^{-1} remains practically constant in the CTS/HcAc spectrum.

3.5. Differential scanning calorimetry (DSC) studies

The DSC curves, presented in Fig. 7, show an endothermic signal at 70 °C observed for commercial CTS, due to the non bonded water loss and an exothermic peak at 322 °C corresponding to the decomposition of amine groups bonded to glucopyranose units [19,20]. The sample CTS-TW is consisting in micro- and nano-CTS structures favored by the presence of 2% v/v Tween-80 and 0,2% v/v oleic acid additives and presents a broad endothermic signal at 55 °C due to the non bonded water loss from the sample.

The sample presents also a weak exothermic signal between 120–210 °C around flashpoint of tween (113 °C) and of oleic acid (~189 °C). On going from 290 °C the decomposition process starts.

Table 2
The maxima in the emission spectra for pure and assembled drugs in solid samples.

Sample	Emission bands (nm)
ASA	320.6
DCF-Na	276.9, 410.2
HcAc	278, 409.2
CTS	277, 409;
CTS/ASA_s	276.7, 431.6
$CTS/DCF\text{-}Na_s$	276.9, 410.2
$CTS/HcAc_s$	276.6, 409.2

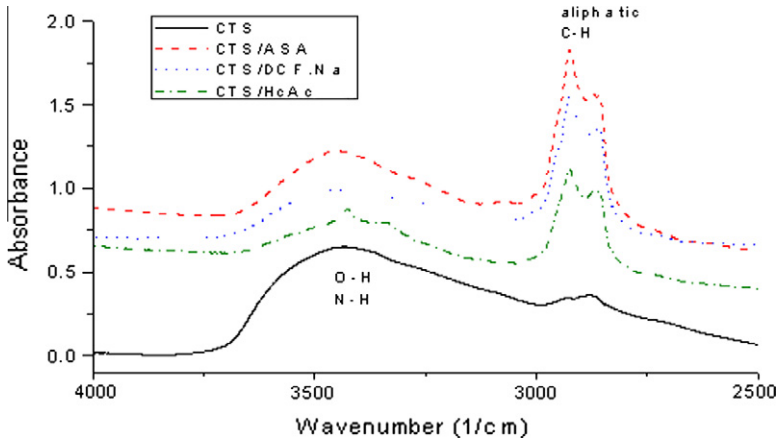

Fig. 5. FTIR spectra of CTS/drug, 4000–2500 cm^{-1} spectral domain.

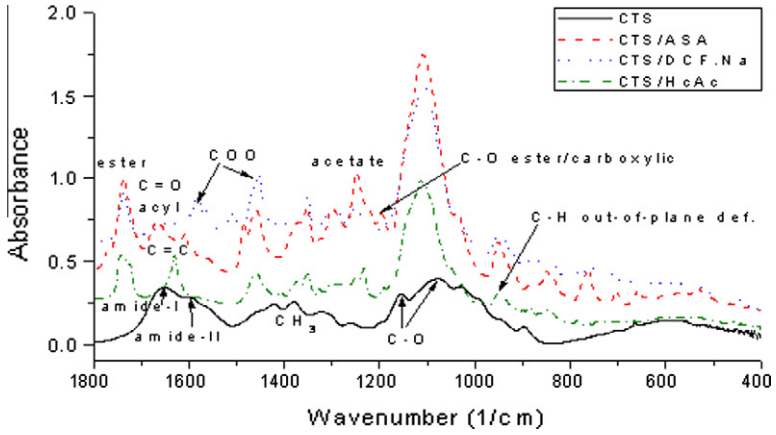

Fig. 6. FTIR spectra of CTS/drug, 1800–400 cm^{-1} spectral domain.

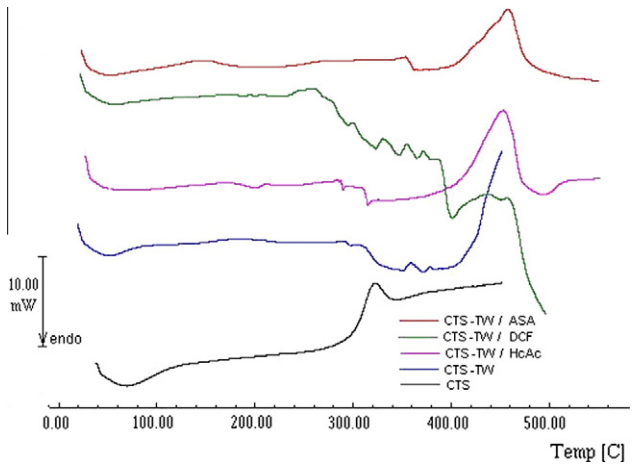

Fig. 7. DSC thermograms of chitosan-anti-inflammatory drug formulations.

The pure drugs melting points by literature data: DCF-Na melting at 287 °C followed by decomposition [21], ASA melting with decomposition between 133–135 °C [22,23] and HcAc melting with decomposition at 223 °C [24].

The sample with HcAc presents a broad endothermic signal at 200 °C. On going from 285 °C the decomposition process starts. On the thermogram of CTS/DCF-Na system a weak broad endothermic signal with maximum at 60 °C is observed, due to the water expulsion and from 230 °C the decomposition process starts. DCF is melted at 284 °C with the decomposition. The CTS/ASA thermogram presents a broad endothermic signal at 55 °C, followed by a broad exothermic plateau centered at 148 °C (possible due to the ASA decomposition); around 330 °C the decomposition process starts. All four micro- and nanostructured CTS samples with and without drug included decompose around 300 °C excepting CTS/DCF-Na system for which the decomposition starts at a lower temperature. All thermograms do not show the drug melting temperatures that demonstrates the inclusion of drug inside CTS microspheres.

3.6. ESR studies

All investigated systems were analyzed by ESR spectroscopy in order to determine the existence of free radicals present in the materials. The same quantity of all spectra was analyzed and the corresponding ESR spectra are presented in the Fig. 8. For all investigated samples an ESR signal ($g = 1.99$) formed by a narrow line with 16G line width typically for CTS is obtained.

A possible origin of this line could be attributed to an initial oxidation stage. There are several ESR studies on CTS with different deacylation degrees [25], where an increase of the signal intensity at $g \sim 1.99$ is due to the oxygen presence in the CTS extraction, purifying and deacylation processes.

For each investigated samples we can observe also different g values determined as follows:

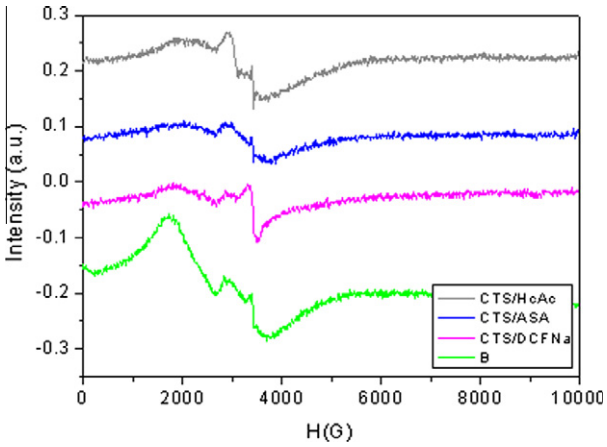

Fig. 8. ESR spectra for analyzed samples.

- CTS/ASA: $g = 2.25$
- CTS/DCF-Na: $g = 2.88$
- CTS/HcAc: $g = 2.35$

Due to the fact that before validation of *in vivo* experiments the biocompatible materials suffer formulation and conditioning processes, it is important to determine structural changes that appear after these procedures.

Consequently, these spongy materials were UV irradiated ($\lambda = 320$ nm) for 4 h; after that ESR experiments were repeated. ESR spectra after irradiation are presented in Figs. 9–11, respectively. As a function of radiation type and its duration, the samples could offer chemical structural changes by chain breaking and the opening of the glycosidic cycles. The drugs present a weak ESR signal at different g values as compared to the starting materials. CTS/DCF-Na material presents a strong signal at $g = 2.14$ that is observed also in DCF-Na spectrum but with a reduced intensity. The irradiation does not produce changes. All investigated materials present the same absorption line at $g \sim 1.99$ but with a higher intensity. This behavior is in good agreement with the literature [20] and could be related to the increase of the free radical concentration of CTS itself.

The analysis of ESR spectra of the active substances before and after irradiation revealed that UV irradiation does not generate free radicals or these radicals are of short life time, irrelevant for eventually structural changes.

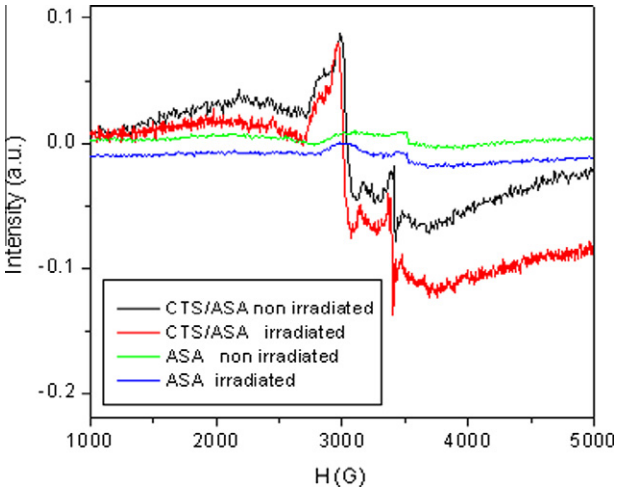

Fig. 9. ESR spectra for ASA and CTS/ASA samples before and after irradiation.

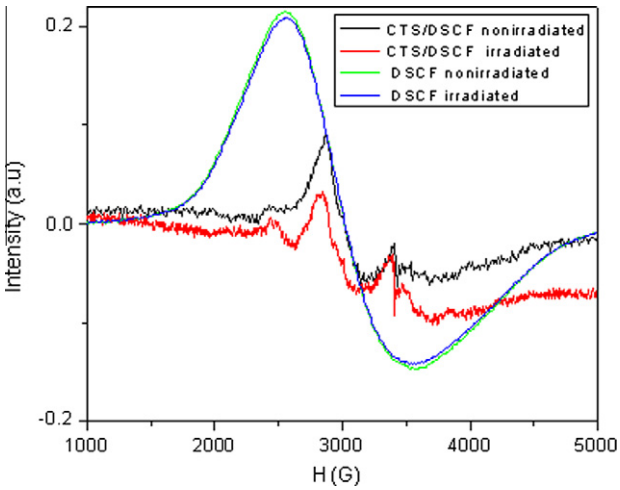

Fig. 10. ESR spectra for DCF-Na and CTS/DCF-Na samples before and after irradiation.

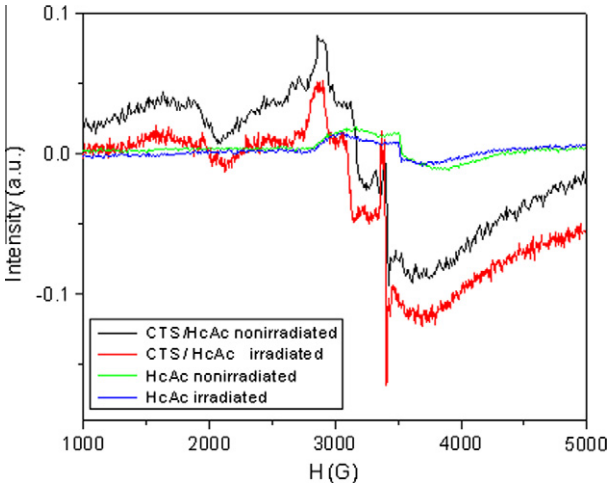

Fig. 11. ESR spectra for HcAc and CTS/HcAc samples before and after irradiation.

The monomer radicals and of CTS polymeric chain are rapidly annihilated due to the concurrent chemical reactions (esterification or amidolyse) which are produced during the supramolecular coupling between CTS (as polymeric chain) and DCF-Na, ASA, or HcAc, respectively, that are more probably in the reaction medium by applying coupling techniques.

3.7. X-ray diffraction

X-ray diffractograms (see Figs. 12–14) show that CTS presents an amorphous structure and in the case of CTS/ASA and CTS/DCF-Na systems the inclusion of the drug does not preserve their crystalline structure (see Figs. 12 and 13). In the case of CTS/HcAc system, due to the higher dimension of this molecule as compared to ASA or DCF ones, the inclusion of HcAc in CTS does not destroy its crystallinity (see Fig. 14).

3.8. Molecular modeling

In order to study the polymer (oligomer) properties of the CTS/ASA and CTS/DCF structures, at least 3–4 CTS-drug units must be included in our molecular geometry structure. These structures usually contain a large number of atoms (over 180 atoms) which

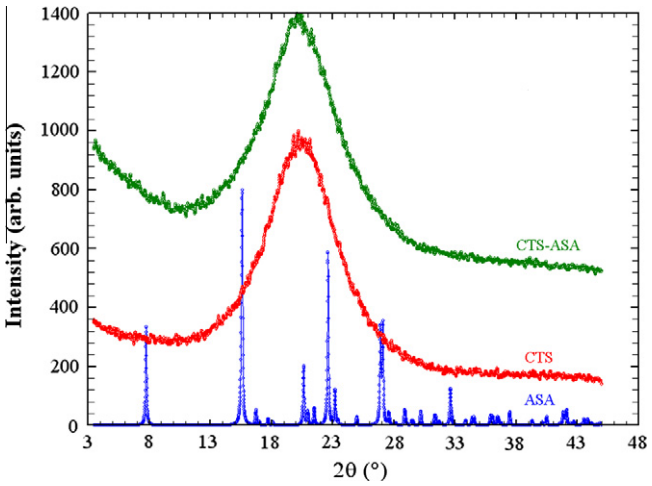

Fig. 12. Diffractograms of ASA/CTS systems.

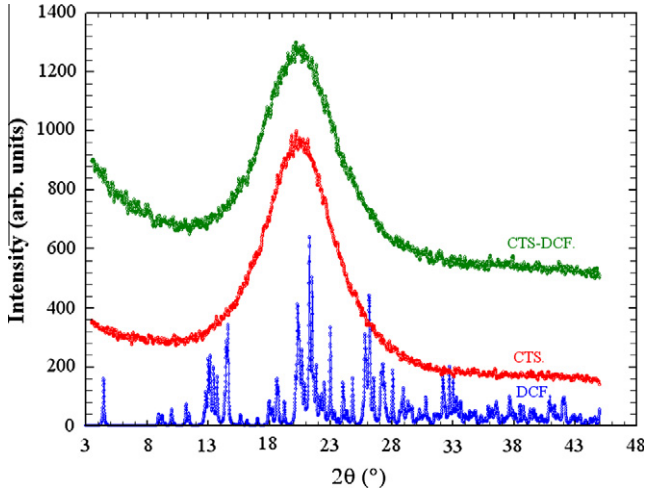

Fig. 13. Diffractograms of DCF-Na/CTS systems.

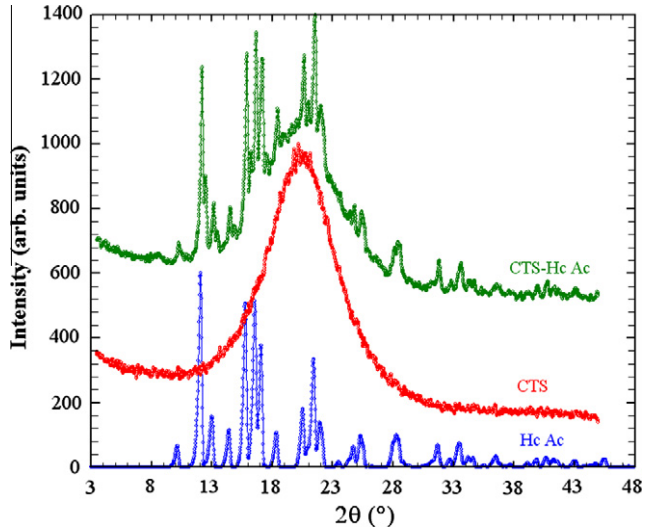

Fig. 14. Diffractograms of HcAc/CTS systems.

could not be properly studied with the conventional *ab initio* or DFT methods, because of the requirement of the huge amount of computer capacity. The density functional-based tight binding method combined with the self-consistent charge technique (SCC-DFTB) [26] can be considered as an adequate solution for treating large biologically interested or nano-scaled molecular materials with nearly good accuracy as it is obtained in case of high level theoretical methods [27–29]. An empirical dispersion correction has also been developed and it was found crucial for predicting reliable nucleic acid base stacking interactions [29], the relative stability of α and 3_{10} helices in proteins [30] and the stability of the double-stranded DNA tetramer with a ligand in the intercalative fashion [31].

By using the SCC-DFTB method [32,33] together with the empirical dispersion correction one can obtain the equilibrium geometry structure of the CTS/ASA and CTS/DCF supramolecular assemblies of four-unit oligomer chain, see Figs. 15 and 16. In both cases one can observe a CTS chain curvature and an orientation of the bioactive molecules toward system inside; the orientation are mainly stabilized by intramolecular hydrogen bonds formed (C═O···H—N or C═O···H—O) between the CTS/ASA (or CTS/DCF) molecular units as well as by the C—H···π bonds between the CTS chain and ASA (or DCF) drug unit. In the case of CTS/DCF system an extra $\pi\cdots\pi$ interaction between the second aromatic rings of DCF could also be observed which stabilizes better the CTS/DCF polymer chain than the CTS/ASA one. Both of C—H···π and $\pi\cdots\pi$ bond formations are as a consequence of the dispersion attractive effects which were included in our model through the empirical correction to the interaction [29].

4. Conclusions

Based on physical–chemical analyses it was demonstrated that:

- Nanostructured and microstructured hydrogels (n-CTS and respectively μ-CTS) were prepared.
- CTS matrix can include anti-inflammatory drugs such as ASA, DCF or HcAc.
- Based on spectrofluorimetry data, one can estimate that the binding between CTS and ASA or DCF-Na are dominantly chemical and physical for HcAc, respectively.
- All investigation methods suggest that different assembling methods depend on the molecular dimension of the molecule that is included in CTS matrix and on its structure.
- A typical CTS signal was observed in ESR measurement consisting in a narrow line formed at $g = 1.99$ A possible origin of this line could be attributed to a initial oxidation stage.
- Analyzing the ESR spectra of the active substances before and after irradiation one can observed that UV irradiation does not generate free radicals or these radicals are of short life time, irrelevant for eventually structural changes.
- Molecular modeling using the density functional-based tight binding method combined with the self-consistent charge technique (SCC-DFTB) one can observe a CTS chain curvature and an orientation of the bioactive molecules toward system inside; the orientation are mainly stabilized by intramolecular hydrogen bonds formed (C═O···H—N or C═O···H—O) between the CTS/ASA (or CTS/DCF) molecular units as well as by the C—H···π bonds between the CTS chain and ASA (or DCF) drug unit. In the case of CTS/DCF system an extra $\pi\cdots\pi$ interaction between the second aromatic rings of DCF could also be observed which stabilizes better the CTS/DCF polymer chain than the CTS/ASA one.

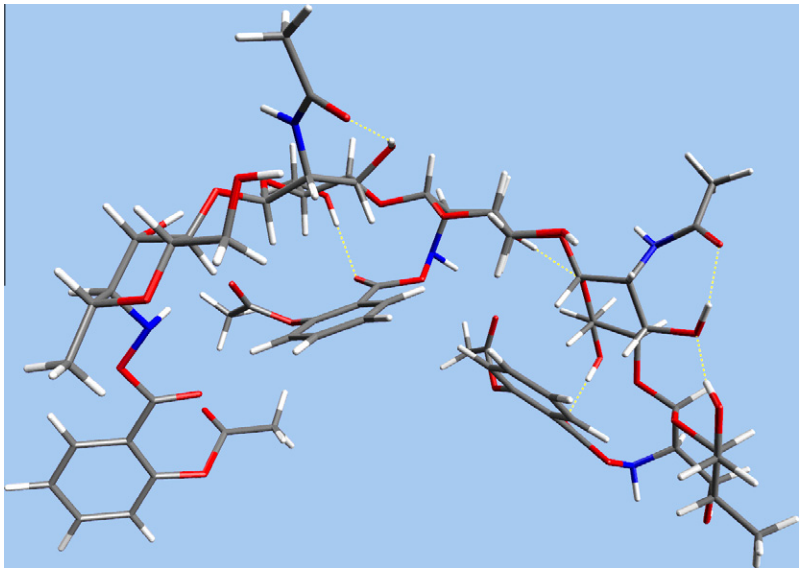

Fig. 15. Model of CTS/ASA assembly.

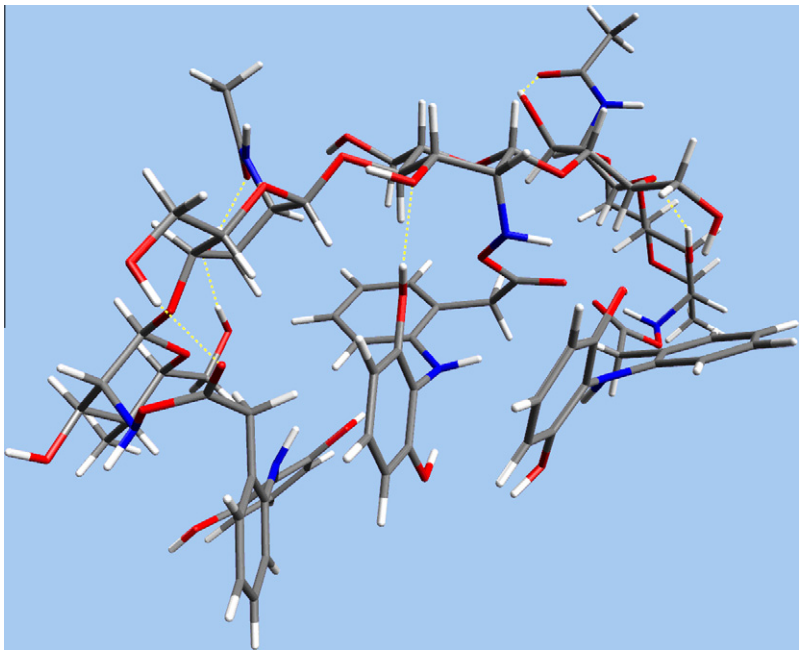

Fig. 16. Model of CTS/DCF-Na assembly.

– All analysis demonstrates that aspirin and sodium diclofenac are better included in chitosan matrix than hydrocortisone acetate, and all the analytical methods used suggested that the nature of the bonds between chitosan matrix and guest molecule are depending on the molecular weight of guest molecule and on the reciprocal stereochemistry of the partners in the system.

Acknowledgments

This work was possible due to the financial support of the Romanian Research and Education Ministry under PN-09-44 02 01/2009, PN-09-44 02 05/2009 and PN II 72-190/2008 projects. We gratefully acknowledge to Data Center of National Institute for Research and Development of Isotopic and Molecular Technologies Cluj-Napoca for providing computer facilities for the molecular modeling calculations.

References

[1] P. Ehrlich, Collected Papers of Paul Ehrlich: Immunology and Cancer Research, Pergamon Press, London, 1902.
[2] I. Szelenyi, K. Thiemer, Arch. Toxicol. 41 (1978) 99.
[3] J.A. Ko, H.J. Park, S.J. Hwang, J.B. Park, J.S. Lee, Int. J. Pharm. 249 (2002) 165.
[4] E.V. Svirshchevskaya, L.G. Alekseeva, P.D. Reshetov, N.N. Phomicheva, S.A. Parphenyuk, A.V. Ilyina, V.S. Zueva, S.A. Lopatin, A.N. Levov, V.P. Varlamov, Eur. J. Med. Chem. 44 (2009) 2030.
[5] K.C. Gupta, M.N. Ravi Kumar, Biomaterials 21 (2000) 1115.
[6] C.S. Sweetman (Ed.), Martindale: The Complete Drug Reference, 33rd ed., Pharmaceutical Press, London, 2002 (Chapter 3).
[7] V.R. Sinha, A.K. Singla, S. Wadhawan, R. Kaushik, R. Kumria, K. Bansal, S. Dhawan, Int. J. Pharm. 274 (2004) 1.

[8] T. Peng, K.D. Yao, Y. Chen, M.F. Goosen, J. Polym. Sci. Polym. Chem. Ed. 32 (1994) 591.
[9] J. Kevin, M.D. Ivey, Am J. Med. 84 (1988) 41.
[10] M.E. Palomo, M.P. Ballesteros, P. Frutos, J. Pharm. Biomed. Anal. 21 (1999) 83.
[11] C. Pinto, R. Neufeld, A. Ribeiro, F. Veiga, Nanomedicine 2 (2006) 53.
[12] N. Anton, J.P. Benoit, P. Saulnier, J. Control Release 128 (2008) 185.
[13] Alina Sionkowska, J. Photochem Photobiol., B: Biology 82 (1) (2006) 9.
[14] J.L. Atwood, J.W. Steed (Eds.), Encyclopedia of Supramolecular Chemistry, Marcel Dekker, New York, 2004 (Chapter 3).
[15] M. Montalti, A. Credi, L. Prodi, M. Teresa Gandolfi, Handbook of Photochemistry, 3rd ed., Taylor &Francis Group, Boca Raton, 2006 (Chapter 5).
[16] N.B. Colthup, L.H. Daly, S.E. Wiberley, Introduction to Infrared and Raman Spectroscopy, Academic Press, New York, 1975.
[17] N. Kourkoumelis, M.A. Demertzis, D. Kovala-Demertzi, A. Koutsodimou, A. Moukarika, Spectr. Acta. A 60 (2004) 2253.
[18] S. Dreve, I. Kacsó, I. Bratu, E. Indrea, J. Phys. Conf. Series 182 (2009), doi:10.1088/1742-6596/182/1/012065.
[19] R.J. Mesley, Spectr. Acta 22 (1966) 889.
[20] G.L. Simionatto, C.É.T. Gomes, Thermochim. Acta 444 (2) (2006) 128.
[21] I. Pasquali, R. Bettini, F. Giordan, J. Therm. Anal. Calorim. 90 (3) (2007) 903.
[22] George D. Beal, Chester R. Szalkowski, J. Am. Pharm. Assoc. 22 (1) (1933) 36.
[23] G.L. Perlovich, A. Bauer-Brandl, J. Therm. Anal. Calorim. 63 (2001) 653.
[24] http://www.caslab.com/Hydrocortisone_acetate_CAS_50-03-3/ http://www.sigmaaldrich.com/catalog/ProductDetail.do?lang=en&N4=H4126|SIGMA&N5=SEARCH_CONCAT_PNO|BRAND_KEY&F=SPEC.
[25] J. Estrela dos Santos, E.R. Dockal, É.T.G. Cavalheiro, J. Thermal. Anal. Calorim. 79 (2005) 243.
[26] M. Elstner, D. Porezag, G. Jungnickel, J. Elsner, M. Haugk, T. Frauenheim, S. Suhai, G. Seifert, Phys. Rev. B 58 (1998) 7260.
[27] M. Elstner, K.J. Jalkanen, M. Knapp-Mohammady, T. Frauenheim, S. Suhai, Chem. Phys. 256 (2000) 15.
[28] M. Elstner, K.J. Jalkanen, M. Knapp-Mohammady, T. Frauenheim, S. Suhai, Chem. Phys. 263 (2001) 203.
[29] M. Elstner, P. Hobza, T. Frauenheim, S. Suhai, E. Kaxiras, J. Chem. Phys. 114 (2001) 5149.
[30] H.Y. Liu, M. Elstner, E. Kaxiras, T. Frauenheim, J. Hermans, W.T. Yang, Proteins: Struct. Funct. Genet. 44 (2001) 484–489.
[31] T. Kubař, P. Jurečka, J. Černý, J. Řezáč, M. Otyepka, H. Valéds, P. Hobza, J. Phys. Chem. A 111 (2007) 5642.
[32] DFTB+ 1.0.1 is a DFTB implementation, which is free for noncommercial use. For details, see <http://www.dftb-plus.info>.
[33] B. Aradi, B. Hourahine, T. Frauenheim, J. Phys. Chem. A 111 (26) (2007) 5678.